BIOCHEMISTRY
including biophysical chemistry & molecular biology

Article

pubs.acs.org/biochemistry

The Zinc Balance: Competitive Zinc Metalation of Carbonic Anhydrase and Metallothionein 1A

Tyler B. J. Pinter[†] and Martin J. Stillman*[,†,‡]

[†]Department of Chemistry and [‡]Department of Biology, The University of Western Ontario, London, Ontario, Canada N6A 5B7

Supporting Information

ABSTRACT: The small, cysteine-rich metallothionein family of proteins is currently considered to play a critical role in the provision of metals to metalloenzymes. However, there is limited information available on the mechanisms of these fundamentally important interactions. We report on the competitive zinc metalation of apocarbonic anhydrase in the presence of apometallothionein 1A using electrospray-ionization mass spectrometry. These experiments revealed the relative affinities of zinc to all species in solution. The carbonic anhydrase is shown to compete efficiently only against $Zn_{5-7}MT$. The calculated equilibrium zinc binding constants of each of the 7 zinc metallothionein 1A species ranged from a high of ($\log(K_F)$) 12.5 to a low of 11.8. The 8 equilibrium constants connecting the 10 active species in competition for the zinc were modeled by fitting the K_F values of the 8 competitive bimolecular reactions to the ESI-mass spectral data. These modeled K values are shown to be experimentally connected to the metalation efficiency of the carbonic anhydrase. The series of 7 metallothionein binding affinities for zinc highlight the buffering role of zinc metallothioneins that permit simultaneously zinc storage and zinc sensing. Finally, the significance of the multiple zinc binding affinities of zinc metallothionein is discussed in relation to zinc homeostasis.

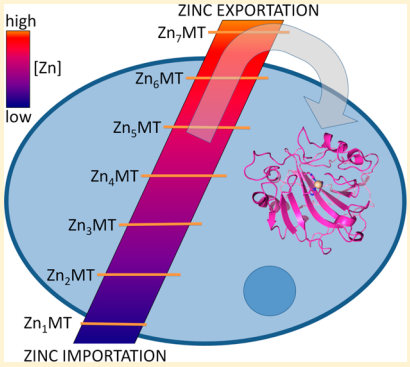

Zinc is the most abundant metal cofactor found in metal-dependent enzymes, with nearly a quarter of identified metalloproteins containing one or more zinc atoms.[1,2] Despite this ubiquity, free zinc levels are tightly controlled.[3,4] The homeostatic intracellular concentration of free zinc is buffered within a narrow range using a symphony of zinc specific sensors, importers, exporters, and chaperones.[5−7] These complex systems work together not only to maintain control of the transport and storage of zinc[8,9] but also to deliver and insert zinc atoms into newly synthesized zinc enzymes.[10−12] When this careful balance of zinc is disturbed, a large number of health complications arise.[13−15] Zinc has also been shown to act as a transcription cofactor and has important roles in cell signaling, development, and proper cellular function.[16,17]

Metallothionein (MT) is a ubiquitous family of metal-binding proteins that are critical to the homeostatic control of cellular zinc (and other metal) levels. Since MT was discovered it has been implicated in toxic metal detoxification, oxidative stress response, and essential metal homeostasis.[18,19] It is capable of binding multiple metals using the relatively high number of cysteine residues for its small size. There are four known human MT isoforms: the more common MT1 and MT2 are predominantly expressed in the liver and kidneys but are also expressed in numerous tissues and cell types; MT3 and MT4 are minor isoforms specifically expressed in specialized tissues such as the brain and epithelial cells, respectively.[20] Numerous MT1 subisoforms have also been identified. MT1 and MT2 are associated with binding both zinc and cadmium *in vivo*.

Human MTs bind up to 7 zinc atoms in tetrahedral ($ZnS_{4(CYS)}$) clusters using 20 cysteines. The fully zinc-saturated Zn_7hMT1A binds the zinc in two distinct domains.[21] The N-terminal beta domain binds 3 zincs using 9 cysteines, and the C-terminal alpha domain binds 4 zincs using 11 cysteines. There are numerous studies on the structure and properties of fully saturated MT's but little information on the important partially metalated species.[22−24] Of particular interest is the relevance of these species to the donation of zinc from MT to zinc-dependent apoenzymes.

MT has been identified as a key player in zinc homeostasis and interacts with numerous metalloproteins.[25] Critical to the *in vivo* functions of MT species is the zinc occupancy of the available metal binding sites. The ability of MT to act as both a zinc donor and acceptor depends on the intracellular zinc (and MT) concentration of the cell. Zn_7MT has been shown to act as a zinc donor to numerous zinc-dependent enzymes, while apoMT is capable of removing and accepting zinc from holo-Zn enzymes.[26,27]

With respect to the role of MT in donating Zn to enzymes, very little has been reported on the mechanistic detail of these important reactions. However, the property of MT acting as a zinc chaperone in the acquisition of free metals and the subsequent release of zinc to metalloenzymes has been previously investigated.[28−33] Carbonic anhydrase has been

Received: July 14, 2014
Revised: September 8, 2014
Published: September 10, 2014

   dx.doi.org/10.1021/bi5008673 | *Biochemistry* 2014, 53, 6276−6285

shown to accept donation of a single zinc atom from zinc-saturated MTs at rates and concentrations that support *in vivo* zinc donation as a function of MT.[32] These studies have shown that fully saturated Zn-MT is capable of donating zinc to the apoenzymes, but the important mechanistic details are not understood.

Carbonic anhydrase (CA), the first discovered metalloenzyme, binds a single zinc atom in its active site using three histidine ligands. CA binds zinc relatively strongly[34] with an apparent stability constant ($\log(K_F)$) of approximately 11.4 at pH 7.[35] Following *de novo* protein synthesis, apocarbonic anhydrase must acquire and insert the enzymatically necessary zinc atom into the active site. However, the estimated femto-^{4} to picomolar[36] pool of "free zinc" is an inadequate zinc source for metalloenzymes to metalate within a suitable time frame,[37] and thus, the majority of the zinc must be acquired from zinc chaperones, of which ZnMT is one example. *In vivo*, numerous zinc sources, chaperones, and enzymes will be in constant competition for the limited amount of zinc within the cell. The range of zinc binding stability constants reported for zinc importers and exporters provides an approximation of the relative range over which zinc is buffered within the cytoplasm. Though exact values are currently not known, there is evidence that zinc importation starts at picomolar concentrations.[38] Exportation of excess zinc is complicated by cellular processes that are designed to protect the cell from metal toxicity, but significant cellular disruptions arise when cells are treated with zinc above 30−100 μM.[39] The K_f values for MT1A zinc binding, as determined by MT-MT competition, apparently fall within the buffering range of functional cells.[40,41]

Studies by numerous groups have shown that Zn_7MT transfers a single zinc atom to CA.[26−28] Zn_7MT and apoMT have been shown to exchange metals with cadmium substituted CA, hypothesized through a protein−protein interaction.[42] However, little is known about the interactions between the apo or partially metalated MT and the apoCA. Since MT exists in a number of partially metalated states,[43] a complete understanding of these interactions is critical to determine the exact mechanistic details of the vitally important metalation reaction of CA.

Recently, our group has reported data[44,45] addressing possible binding motifs for the partially metalated recombinant human MT1A (rhMT1A), but no experimental data have been reported that specifically describe the mechanism for zinc transfers from these partially metalated MTs. The conclusion from the binding motif studies was that a beaded 5 zinc structure formed initially; addition of further zinc resulted in the development of a clustered two domain structure containing the full complement of 7 zinc ions. The consequence of this result was that the last two zinc ions bound with lower binding constants, and it was suggested that these two zinc ions would be accessible for donation to apoenzymes.[46]

In this paper, we report on the zinc titration of rhMT1a in the presence of carbonic anhydrase. Apocarbonic anhydrase, which remains folded following loss of zinc,[47] acts as a putative model for understanding the homeostatic control of zinc with respect to the metalation of zinc enzymes. We report the metalation status of CA and rhMT1A during a competitive titration with zinc and have determined the relative stability constants for each of the 7 independent MT-bound zinc ions with respect to the single zinc stability constant for CA. The data indicate that CA outcompetes rhMT1A for the 3 weakest bound zinc atoms and shows little competition for the first four zinc bound by rhMT1A. Finally, we discuss the homeostatic control of zinc concentrations to demonstrate the suitability of MTs as a zinc reservoir for apo zinc-dependent enzymes.

EXPERIMENTAL PROCEDURES

Preparation of apoMT. rhMT1A was expressed and purified following previously reported methods.[48] The MT sequence used in this study is based on the recombinant human MT1A sequence that consists of 72 residues: MGKAAAACSC ATGGSCTCTG SCKCKECKCN SCKKAAAACC SCCPMSCAKC AQGCVCKGAS EKCSCCK KAA AA. The corresponding DNA sequence was inserted as an N-terminal S-tag (for protein stability purposes) fusion protein into a pET29a plasmid and expressed in BL21(DE3) *E. coli* cells as Cd_7MT. All solutions were rigorously evacuated and argon saturated to impede cysteine oxidation. Following protein purification, the S-tag was removed with a Thrombin CleanCleave Kit (Sigma). Concentrated HCl was used to adjust the pH to 2.7 before apoMT was separated from the cadmium using SEC on GE Sephadex G-25 size exclusion media using 5 mM formic acid pH 2.7 buffer as the eluent. The deoxygenated apoMT was simultaneously concentrated and buffer exchanged to pH 7.0 using Millipore Amicon Ultra-4 centrifuge filter units under argon (3 kDa MWCO).

Preparation of apoCA. Bovine CA (Sigma) was first purified on a Sephadex G-50 gel filtration column with 5 mM pH 7.4 ammonium formate buffer as the eluent. The fractions containing only pure carbonic anhydrase 2 were pooled and concentrated with 10 kDa MWCO Amicon centrifuge filter units. The zinc was removed from the CA through modification of methods previously reported.[49] An equal amount of 50 mM 2,6-pyridinedicarboxylic acid pH 6 (PDA) was added to the concentrated CA and spun down in the filter unit. The PDA zinc wash was repeated 6 times. To remove PDA from apoCA prior to MS experiments, the protein was exhaustively buffer exchanged to 5 mM ammonium formate pH 7.4 until neither PDA nor zinc were detected in the filtrate.

ESI-MS Procedures. Stock apo-rhMT1A concentrations were determined by remetalation of a small fraction of protein with Cd^{2+}; formation of Cd_7MT was monitored through the 250 nm thiolate-to-cadmium charge transfer band, $\varepsilon(250)$ = 89,000 M^{-1} cm^{-1}. Stock apoCA concentrations were determined using $\varepsilon(280)$ = 45,000 $M^{-1}cm^{-1}$. Zinc acetate stock (10 mM) was prepared in deionized water; all molar equivalents of zinc were determined through atomic absorption spectroscopy. Equal concentrations of both stock apoproteins were mixed in a vial, and equivalents of zinc were added under argon atmosphere and allowed to equilibrate for a minimum of 3 min between addition and data collection; separate samples were left for up to 1 h (data not shown), and there was no change in zinc distribution with longer incubation times. ESI mass spectral data were collected on a Bruker Micro-TOF II (Bruker Daltonics, Toronto, ON) operated in the positive ion mode calibrated with NaI. Settings: scan = 500−4000 m/z; rolling average = 2; nebulizer = 2 bar; dry gas = 80 °C @ 6.0 L/min; capillary = 4000 V; end plate offset = −500 V; capillary exit = 175 V; Skimmer 1 = 30.0 V; Skimmer 2 = 23.5 V; Hexapole RF = 800 V. The spectra were collected for a minimum of 2 min and deconvoluted using the Maximum Entropy (Max Ent) application of the Bruker Compass DataAnalysis software package. All titrations were performed

dx.doi.org/10.1021/bi5008673 | *Biochemistry* 2014, 53, 6276−6285

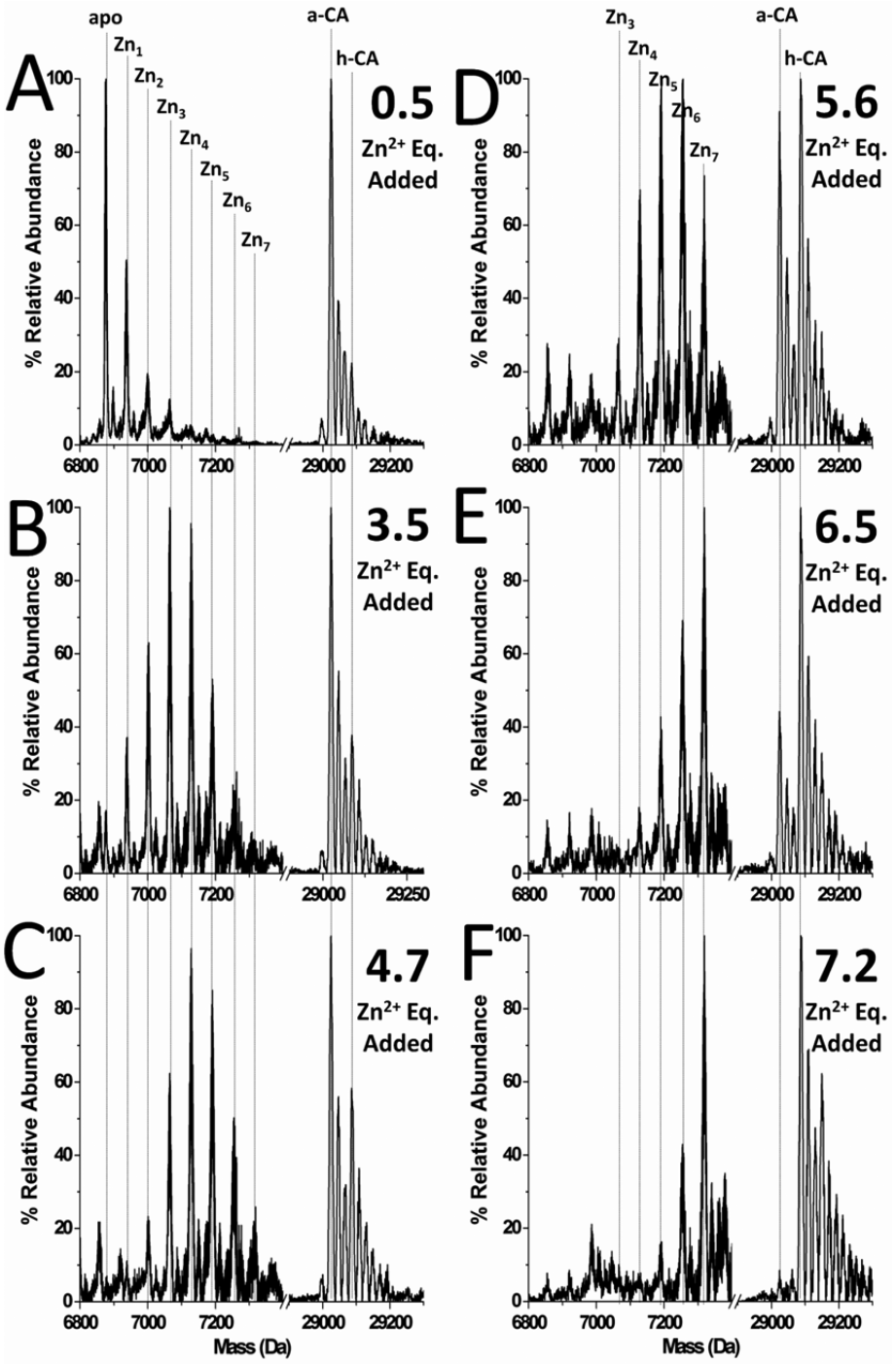

Figure 1. Deconvoluted ESI mass spectral data recorded for the equimolar competitive titration of apo-CA and apo-rhMT at pH 6.8. The apoproteins were mixed to a final concentration of 30 μM under argon. Zinc (1 mM in diH_2O) was aliquoted into the solution of the combined proteins. The sample was equilibrated for 3 min on ice before signal acquisition. The zinc speciation of the MT and CA is highlighted with vertical gray lines. The mass range for each species has been normalized to 100% relative abundance.

in at least triplicate to ensure accuracy and reproducibility of results.

RESULTS

Figure 1 shows a selection of the deconvoluted mass spectral data recorded during a competitive zinc titration to a solution containing equal concentrations of apo-rhMT1A and apoCA. The deconvoluted data shown here were calculated from the charge state spectra in Figure S1. This Figure shows the formation of the fully metalated Zn_7MT and ZnCA (F) as a function of six representative steps of the titration (A–E). The abundance of each species was plotted relative to the most abundant species of the protein: apoMT and apoCA in Figure 1A, and Zn_7MT and holoCA in Figure 1F. Zinc equivalents were determined from the concentration of the two proteins and AAS measurements of the zinc solution. These equivalents refer to a ratio such that 1 zinc equivalent would fill a single zinc binding site. Therefore, 8 zinc equivalents (7 for MT and 1 for CA) are required to fill all the sites, completing the titration.

dx.doi.org/10.1021/bi5008673 | *Biochemistry* 2014, 53, 6276–6285

The relative concentrations of each metalated species were plotted in Figure 2 as a function of the equivalents of zinc

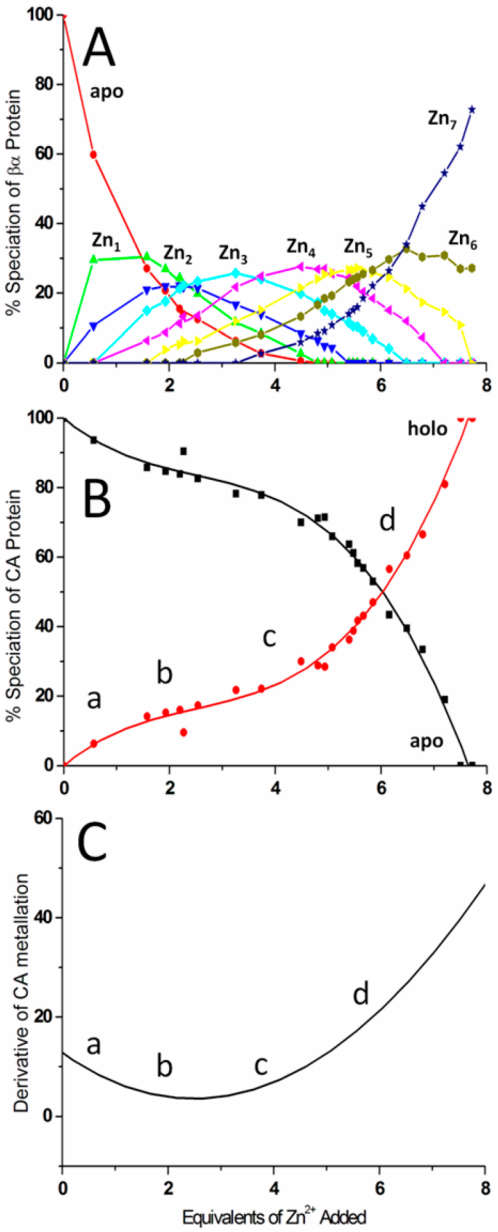

Figure 2. Experimentally determined zinc status of MT (A) and CA (B) during the stepwise competitive zinc metalation based on the ESI mass spectral data partially shown in Figure 1. Figure C shows the metalation efficiency of CA calculated as the first derivative (d[apoCA]/d[Zn^{2+} added]).

added stepwise. The individual zinc metalated species were extracted from the mass spectral data. Figure 2A shows the experimental data for the 8 rhMT1A species (apoMT to Zn_7MT). Figure 2B shows the corresponding experimental data for apoCA and ZnCA, as a function of the equivalents of zinc added. The CA was 50% metalated when 6 equiv of zinc was added. The change in the zinc binding efficiency of apoCA is shown in Figure 2C as the first derivative (d[apoCA]/d[Zn Added]) of the metalation of the apoCA line shown in Figure 2B. We will return to discuss the significance of the data representations in Figure 2C below.

In order to determine the zinc binding affinity for each of the rhMT1A species, the metalation state at each specific zinc loading was simulated from a model that minimized the root-mean-square difference between the experimental and a theoretical data set determined by the 8 binding constants. The model was based on 7 sequential bimolecular reactions that resulted in the formation of Zn_7MT from apoMT and the competitive reaction of apoCA forming ZnCA. The relative concentrations of each species depend on the relative binding constants (K_{MT1-7} and K_{CA1}).

Figure 3 shows a fit of the apo-rhMT1A and apoCA experimental ESI mass spectral data using 7 consecutive

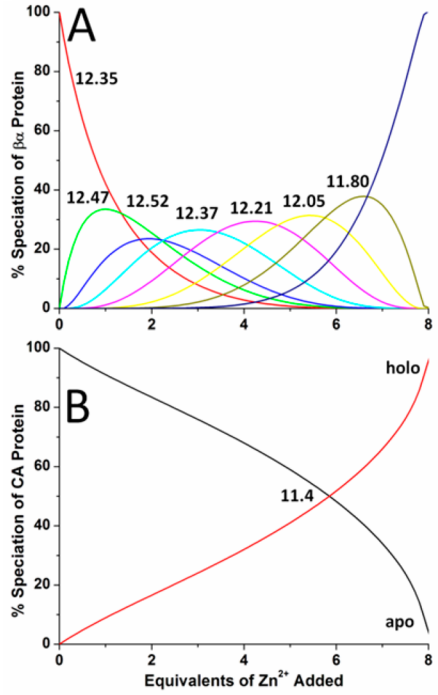

Figure 3. Simulation of the competitive zinc metalation of apo-MT (A) in the presence of apoCA (B). The simulation uses $\log_{10}(K_F)$ values for the MT of 12.35, 12.47, 12.52, 12.37, 12.21, 12.05, and 11.80 for the 7 sequential metalation events in the formation of Zn_7MT. These values were derived from extraction of the competition speciation of the MT versus the known $\log_{10}(K_F)$ of CA of 11.4. The simulations reported in (A) were developed from methods first described by Sutherland, et al. for zinc metalation of MT.[45]

equilibrium binding constants for the apoMT coupled to the single metalation equilibrium for the apoCA. The simulated competition reaction used the following criteria: (i) the log K_F of CA is 11.4 under the conditions of the experiments,[35] and (ii) all reactions were coupled and reversible such that zinc could freely redistribute to the preferred occupancy. This model was used to simulate the speciation profiles shown in Figure 2 to allow direct assessment of the accuracy of the fits. The 7 K_F values for MT zinc binding, determined by the model, which most closely fit the experimental data, were log-[$K_{F(1-7\ Zn)}$]: 12.35, 12.47, 12.52, 12.37, 12.21, 12.05, and 11.8.

In Figure 3A the stepwise metalation of rhMT1A proceeds through 6 distinct intermediates between apoMT and Zn_7MT. Figure 3B shows the simulated metalation of apoCA as a function of increasing concentration of zinc. There is very close alignment between the simulated data in Figure 3A and the experimental data in Figure 2A for the metalation of MT and

dx.doi.org/10.1021/bi5008673 | *Biochemistry* 2014, 53, 6276−6285

between the simulated data of Figure 3B and the experimental data from Figure 2B for the metalation of CA. Figure S2 shows the overlaid model and experimental traces for assessment of the quality of the fit. Because the set of 8 K values is determined in a single calculation, we have confidence that the K values determined in the model represent accurate values under the conditions of the experiment. It should be noted that the individual values of each K_n (n = 1−7) impact the quality of the fit for all other species, since the equilibrium equations are all coupled and successive while also being in competition with each other and the CA. The experimental error on all reported K values by the model is on the order of ±0.3 log units. An overlay of each individual species fit and experimental data is shown in Figure S2 for comparison. It should be noted that since the model minimized the error and provided a fit for all 10 speciation traces (apo to Zn_7MT and apo and holoCA) simultaneously that not all the model traces exactly match the data; Zn_5- and Zn_6MT, for example, show some deviation between the model and experimental data.

Sequential Metalation Reactions for the Competitive Titration of Zinc to apoMT and apo-CA

$$\text{Apo-}\beta\alpha\text{-rhMT} + Zn^{2+} \overset{K_1}{\rightleftharpoons} Zn_1\text{-}\beta\alpha\text{-rhMT}$$
$$\log(K_1) = 12.35 \quad (1)$$

$$Zn_1\text{-}\beta\alpha\text{-rhMT} + Zn^{2+} \overset{K_2}{\rightleftharpoons} Zn_2\text{-}\beta\alpha\text{-rhMT}$$
$$\log(K_2) = 12.47 \quad (2)$$

$$Zn_2\text{-}\beta\alpha\text{-rhMT} + Zn^{2+} \overset{K_3}{\rightleftharpoons} Zn_3\text{-}\beta\alpha\text{-rhMT}$$
$$\log(K_3) = 12.52 \quad (3)$$

$$Zn_3\text{-}\beta\alpha\text{-rhMT} + Zn^{2+} \overset{K_4}{\rightleftharpoons} Zn_4\text{-}\beta\alpha\text{-rhMT}$$
$$\log(K_4) = 12.37 \quad (4)$$

$$Zn_4\text{-}\beta\alpha\text{-rhMT} + Zn^{2+} \overset{K_5}{\rightleftharpoons} Zn_5\text{-}\beta\alpha\text{-rhMT}$$
$$\log(K_5) = 12.21 \quad (5)$$

$$Zn_5\text{-}\beta\alpha\text{-rhMT} + Zn^{2+} \overset{K_6}{\rightleftharpoons} Zn_6\text{-}\beta\alpha\text{-rhMT}$$
$$\log(K_6) = 12.05 \quad (6)$$

$$Zn_6\text{-}\beta\alpha\text{-rhMT} + Zn^{2+} \overset{K_7}{\rightleftharpoons} Zn_7\text{-}\beta\alpha\text{-rhMT}$$
$$\log(K_7) = 11.80 \quad (7)$$

$$\text{Apo-CA} + Zn^{2+} \overset{K_{CA}}{\rightleftharpoons} \text{Holo-CA} \qquad \log(K_{CA}) = 11.4 \quad (8)$$

The apparent stability constants for each sequential zinc addition to MT are indicated by $\log(K_n)$ (n = 1−7), and the apparent stability constant for zinc binding to apoCA is indicated by $\log(K_{CA})$. The 7 log K_F values for MT are plotted in Figure 4A as a function of the MT zinc loading in order to compare the magnitudes of the zinc binding constants. While the first 2 constants are below the value of K_{MT3}, the values of K_{MT3} to K_{MT7} follow the expected linear decrease that results from the statistical reduction of available zinc binding sites.

Figure 4B shows the superimposition of the change in binding efficiency of apoCA as a function of the total zinc load

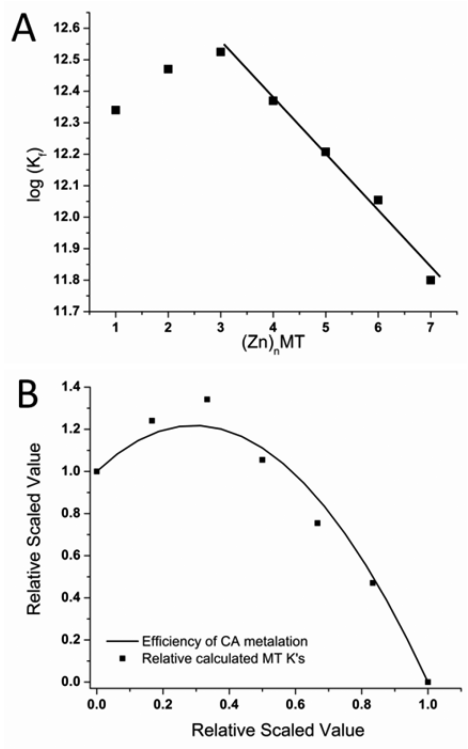

Figure 4. Calculated stability constants (A) and the experimental data reflecting those values (B). (A) The calculated fitted K values of MT that best fit the data shown in Figure 2 to produce Figure 3 based on the competitive metalation of apoMT in the presence of CA. The solid line shows the linear trend of decreasing K values as the MT metalates. (B) Superimposition of the relative metalation efficiency of apoCA (solid line) plotted against the calculated $\log(K_F)$ values (points). The two data sets were scaled such that the initial values (metalation efficiency and first MT zinc binding K) were 1.

inverted from Figure 2C (line) and the binding constants calculated for the 7 zinc rhMT1A species (points) relative to the first K. This figure shows how the experimental data reflect directly the calculated K values for both MT and CA. The importance of this figure is that we observe the precise trend in the value of K values that were calculated in the model from the raw experimental data of the metalation of CA. These data are particularly important in confirming the increase in K_2 and K_3 for the metalation of MT.

Figure 5 shows the experimental (red) mass spectral data at representative zinc additions compared with the simulated (black) mass spectral data predicted by the model shown in Figure 3 above. Parts A−G of Figure 5 show the experimentally determined relative abundance of 7 zinc containing MT species from the full data set. Parts H−N of Figure 5 show the predicted mass spectral data based on the model used in Figure 3 at these same zinc loadings. Parts O−U of Figure 5 show the experimental and predicted mass spectral data again at the same zinc loading values for CA. Only the apo and holo species profiles are shown because CA binds a single zinc.

DISCUSSION

MT is a metallochaperone with the proposed role of supplying zinc to apoenzymes. While numerous studies have discussed the metalation of CA, even including interactions with Zn_7MT, we believe that no studies have previously addressed the mechanism for a potential role of zinc buffering between MT

dx.doi.org/10.1021/bi5008673 | Biochemistry 2014, 53, 6276−6285

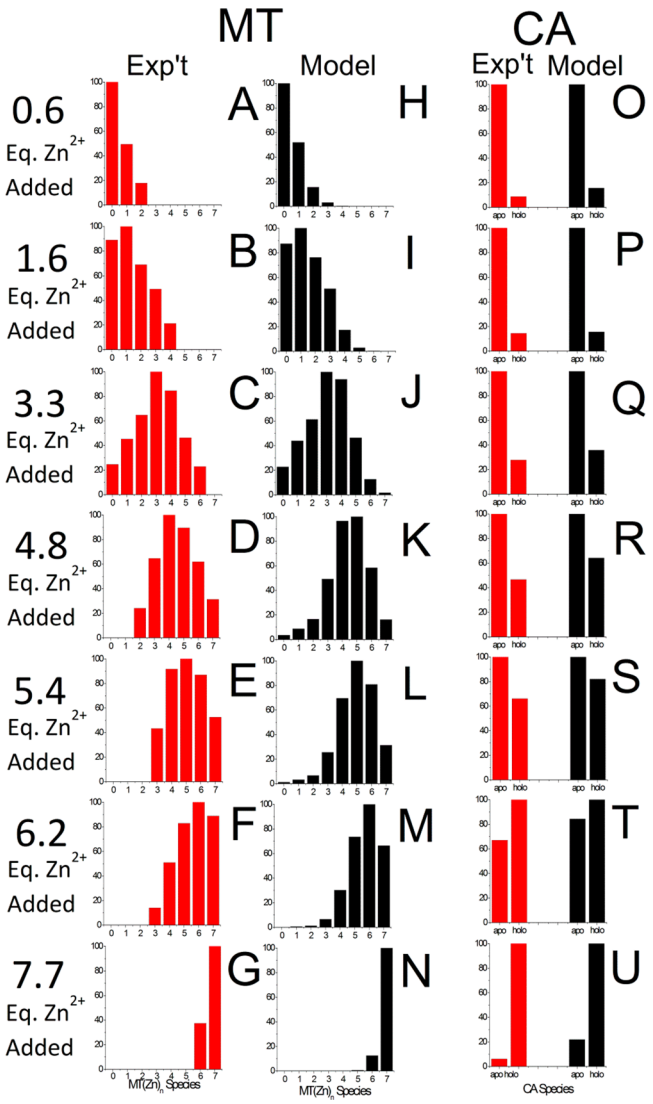

Figure 5. ESI mass spectral data based on experimental data (red) and data produced by simulating the titration using the best fit K_F values (black). A–G show the experimental mass spectral data collected for all Zn_nMT (n = 0–7) species during the competitive titration of apoCA and apoMT. H–N shows the predicted ESI mass spectral data for the same species generated from the simulated titration. O–U shows both the experimental and predicted ESI mass spectral data for apo and holoCA species.

and the apoenzyme. Results from both our lab and Maret et al. indicate that a ladder of binding constants exists for the binding of zinc to metallothionein.[44,50]

Our previous results showed that MT1A possesses 7 independent sequentially decreasing zinc binding affinities from zinc competition experiments between the full rhMT1A protein and individual N-terminal β and C-terminal α domains. Our previous work[44] used a much simpler modeling procedure and manually set the span of the 7 K's to extend over the data reported by Maret and co-workers[50] as a best estimate for the K values. In this current report, the modeling of the K values is locked to the known value of carbonic anhydrase metalation. The model mathematically minimized the errors on the values of K so the model best fits the data. In this way, this current set of K values has both confirmed the existence of the 7 independent zinc binding affinities and calibrated their values to accommodate the known value of CA.

In order to place the metalation of CA within this ladder, we designed an experiment in which both aporhMT1A and apoCA could compete for zinc as it was added in a stepwise manner. The competition experiment is unique in that it is able to leverage the difference in the relative binding affinities for such high affinity sites.[51] In the presence of a competitive zinc binding site, such as that found in CA, the two proteins will redistribute zinc to form the thermodynamically preferred zinc distribution that will be governed by the relative magnitudes of the 8 equilibrium constants. Our data show how apoCA metalates with a sequence directly related to the relative binding constants of the 7 individual sites in MT. This establishes the buffering properties afforded by MT for zinc.

Figure 1A shows how the initial zinc binds in a distributed fashion to the rhMT1A and, to a minor extent, to the CA. The important observation is the change that takes place when a further 3 zinc equivalents are added and the data in Figure 1B recorded. At this point during the titration, the Zn_3 and Zn_4MT species dominate the distribution of zinc metalation, whereas, in contrast, the ZnCA fraction has increased only slightly. These data clearly and unambiguously show that MT is binding a greater fraction of the added zinc than the CA. This can only occur under the equimolar conditions of the competition experiment, if the relative binding constants favor MT zinc binding. Addition of a further 2 zinc equiv (to 5.6 total added; Figure 1D) results in both MT and CA binding significant fractions of the added zinc. This means that the binding site affinities in MT must be more similar to the binding site affinity of CA. The major change in zinc binding to CA occurs with the addition to 6.5 equiv (Figure 1E). Now approximately 70% of the CA is metalated.

Figure 2A clearly shows the stepwise metalation proceeds as reported previously for zinc binding, in that each individual species (meaning Zn_1 to Zn_5) forms and then is replaced with approximately the same fractional composition of about 30% maximum. At each point in the titration, the data here show the distribution of species simply by constructing a fractional distribution. For example, at the 4.0 zinc added point, the slice through the data shows that the relative concentrations are Zn_4 > Zn_3 > Zn_5 > Zn_2 > Zn_6 > Zn_1 > Zn_7 > apoMT.

Figure 2B shows that the binding of zinc to apoCA takes place nonlinearly as a function of zinc added. In the region from 0 to 5 zinc added, the data show that zinc binding to CA is dependent directly on the relative binding constant for the individual sites in MT. This means that, for example, the small fraction of the initial addition of zinc is bound by CA when Zn_1MT is forming. However, when Zn_3MT forms at about 3 zinc added, CA metalation is depressed so that between 3 and almost 5 zinc added only about 5% of the CA metalates, due to the increase in competition from the MT. The CA metalation trend, therefore, mirrors the span of the 7 MT binding affinities: when the binding affinity for CA is closer to that of a single site in MT, CA metalates, but when the binding affinity of CA is much less than MT, MT metalates.

The sensitivity of apoCA metalation to the presence of the 7 competing MT sites can be expressed by taking the derivative of the metalation status of apoCA as a function of the number of added zinc (Figure 2C). From points a to b, the binding affinity difference increases between apoCA and the MT species and CA metalation becomes less efficient with respect to MT metalation ($Zn_{1-3}MT$ bind while CA essentially stops

dx.doi.org/10.1021/bi5008673 | Biochemistry 2014, 53, 6276–6285

binding zinc). In the b−c region, CA metalation is essentially zero (less than 10% change over 3 equiv of zinc added), in contrast to MT metalation of Zn_{2-4}MT. However, the c−d region shows the onset of apoCA metalation; now CA is competing more efficiently against the formation of Zn_{6-7}MT. The unusual region is the pivot point between b−c and c−d because at this point there is a distinct reduction in the binding affinity of the competitive species (Zn_nMT). We interpret this pivot point to represent the threshold in the binding affinities of the MT species with respect to apoCA. This is demonstrated in Figure 2C because if the binding affinities for every MT site were the same, the derivative (d[apoCA]/d[Zn Added]) would be constant for a competitor with the same binding affinity.

The binding affinity data calculated for Figure 3 introduced an interesting trend. Whereas we expected the sequence of binding affinities for MT to diminish, as we noted above, the fits required that K_1 and K_2 should be lower than K_3. The effect of this can be seen in Figure 2B, as described above, where apoCA metalates proportionally with a greater fraction than at the higher zinc-added points. The 7 calculated equilibrium constant values determined for each zinc addition from the competitive titration experiments shown in Figures 1−5 are shown in eqs 1−7 (note that the value of log(K_{CA}) was taken from the literature as 11.4).[35]

The unexpected increase in zinc affinity for the first two binding constants (where K_1 (apoMT) < K_2 (Zn_1MT) < K_3 (Zn_2MT)) could possibly arise from the much greater fluxional nature of the apoMT strand and therefore lack of structured zinc binding sites as compared to the partially metalated (and therefore structured) Zn_1- and Zn_2MT species. The binding of the first and second metal must rearrange the peptide backbone to accommodate metal binding. This rearrangement facilitates the subsequent metalation events (Zn_1- to Zn_2 and Zn_2- to Zn_3MT) in a manner not previously observed due to the fact that multiple species are metalating simultaneously as shown in the modeling and especially the deconvoluted and raw ESI mass spectral data. Once three zinc atoms have been incorporated by the MT strand, this effect is no longer observed, since a majority of the strand now must now possess some organized structure.

We have previously noted this change in structure from the charge state distribution following metalation of the apoMT. For example, this same trend was observed in arsenic binding to MT[52] and may be connected with the globular conformation of apoMT suggested from the ESI mass spectral data.[53] This arsenic work showed that the kinetics of arsenic binding was mostly controlled by the rate of the on reaction (k_{on}), as the rate of the off reaction (k_{off}) for each As_xMT species was presumed to be similar. Since the equilibrium binding constant (K) equals the ratio of (k_{on}/k_{off}) and since the k_{off} values were presumed similar, those kinetic parameters reflect directly the equilibrium binding of arsenic to MT. While the values and magnitudes are certainly not comparable, and even though it used a different metal, these arsenic data highlight the surprising similarity in the trends between these kinetic arsenic data and the zinc equilibrium data described here.

The values of the subsequent K_n (n = 3−7) follow the expected trend for distributed metalation in which the number of sites available diminishes sequentially so that the value of K_n also diminishes. Recent results have shown that even low zinc occupancy MT species (Zn_nMT, where n = 0, 1, or 2) adopt structural characteristics that differ from the traditional view of apoMT's existing as a pure random coil.[54,55]

The span of the 7 stability constants, relative to the apoCA zinc binding constant, shows that MT zinc binding occurs throughout the range of zinc enzyme stability constants, the start of the titration against much higher affinity MT binding sites. As the MT binds zinc sequentially into each site, the binding constants decrease to a point where the apoCA can begin to compete more efficiently with MT for the incoming zinc. CA then continues to compete with MT for the incoming zinc until it saturates, and MT binds the remaining incoming zinc until it too is saturated.

In order to visualize the effects of the relative binding affinities on the zinc distribution, we have included the results of a computational simulation that demonstrates the major changes that take place in the fractional distribution of zinc as a function of the relative magnitudes of the binding affinities of an example metal chaperone (MT) and a metal-dependent enzyme (CA).

For simplicity, we used only a single site competitor, and so the x-axis is just up to 2 zinc added. We explored the effect of the different ratios of the binding affinities and show those results in Figure 6. The panels in Figure 6 examine the effect on the metalation of apoCA for five scenarios: (A) where $K_{comp} < K_{CA}$ by 0.5 log units; (B) where $K_{comp} = K_{CA}$; (C) where $K_{comp} > K_{CA}$ by 0.5 log units; (D) where $K_{comp} > K_{CA}$ by 1 log unit; and (E) where $K_{comp} > K_{CA}$ by 1.5 log units. What is important in this figure is that the trend in the metalation of apoCA for the set of values of binding affinities obtained from the fit reported in Figure 3 can be simulated. Figure 6D shows that competition with a competitor whose zinc binding affinity is approximately 10× stronger than the zinc acceptor results in inefficient metalation until over 50% of the zinc has been bound to the competitor. The trend in apoCA metalation, therefore, illustrates the situation at the different points in Figure 2B. Figure 6A shows metalation taking place efficiently because the competitor binding constant is modeled to be less than that of CA. Clearly, the amount of zinc that is available for an enzyme to acquire from MT is dependent on the relative zinc binding constants. An enzyme with a high zinc binding constant has a much larger zinc pool available than those enzymes that bind zinc more weakly. The series of binding constants represent, in sequence from high to low, the increase in the availability of zinc to a zinc acceptor.

The efficiency in metalation of the apoCA, by which we mean the fraction of the added zinc that apoCA binds compared with the MT, confirms the presence of the multiple binding affinities of the 7 MT sites. This effect is directly dependent on the intricate equilibrium chemistry that takes place when 8 possible binding sites vie for the zinc that is added in a stepwise manner. This is, therefore, a zinc binding landscape within which carbonic anhydrase competes for the zinc needed for its single site. That the binding affinity of apoCA is smaller than the last zinc bound to the MT sets up the buffering action controlled by the 7 sites of MT.

When the cell is in a state of zinc excess, MT production is induced. It would be advantageous for the newly synthesized apoMT proteins to rapidly bind the weakly associated zinc that turn on zinc specific transcription factors such as MTF-1. The first few zinc that are bound to MT, therefore, act as a deep sink of bound zinc. This deep sink is only accessible during times of extreme zinc deficiency. The rest of the zinc binding constants decrease approximately linearly. The more weakly bound zinc act as a shallow source of zinc, to be exchanged between other zinc sinks and enzymes. Our proposal is that MT acts as both a

dx.doi.org/10.1021/bi5008673 | Biochemistry 2014, 53, 6276−6285

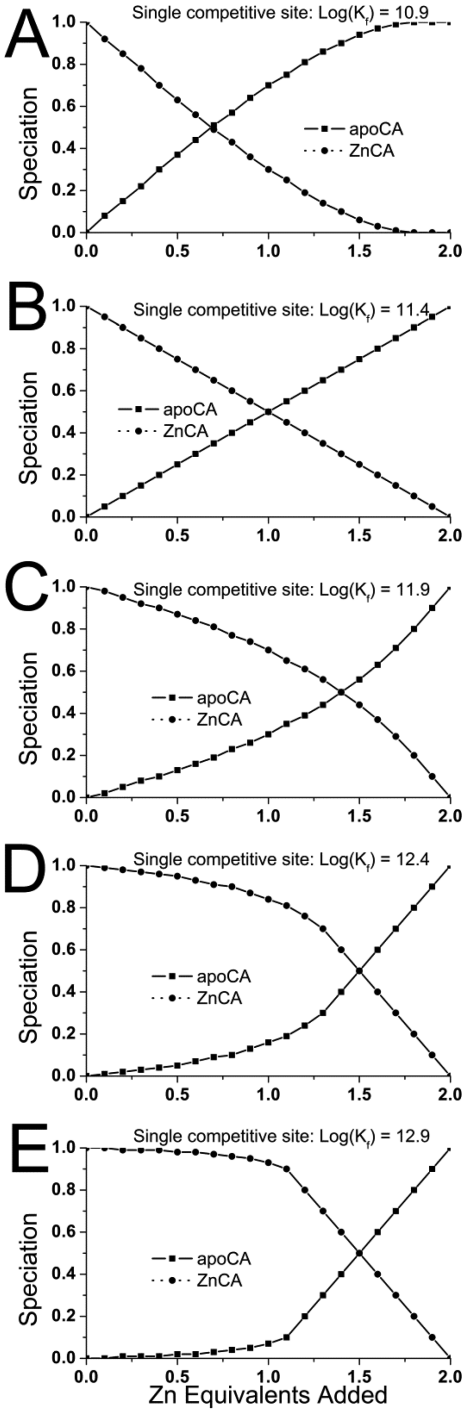

Figure 6. Modeled CA speciation profiles for the simulated competitive zinc titration between CA and a single zinc binding site competitor with zinc affinity increasing by 0.5 log units A (10.9) to E (12.9). The simulated titration requires 2 equiv of zinc to complete. The zinc occupancy of the CA depends on the relative difference in the zinc binding affinity from the competitor. These model traces highlight the sensitivity of our modeling for interpreting speciation and determining relative zinc affinities. Log(K_{CA}) was set to 11.4.

zinc chaperone (one of many others) and a zinc sensor for the cell. When zinc levels are low and the cell is zinc starved, MT binds all available zinc, which has two effects: to turn on zinc importers and to cause upregulation of genes that code for zinc importation. Both would result in the increase of cellular zinc concentration. The facility of zinc-loaded MT to donate occurs when the cell is zinc-loaded and the most predominant MT species have >6 zinc bound. These species supply the weakly bound zinc to zinc-dependent apoenzymes; the most weakly bound zinc ion is also likely constantly exchanging with weak zinc binding sites, highlighting the role of zinc buffering. If the cell contains zinc in excess of the MT binding capabilities, these "free" zinc are bound by nonspecific zinc sites, sequestered into zinc vesicles, and/or bound by and exported by zinc exporters,[56,57] which have lower zinc binding constants. Thus, MT is able to act as a zinc buffer, maintaining the appropriate cellular concentration of zinc by utilizing the range of the zinc binding constants.

In conclusion, in this paper, we show the precise metalation status of both apoCA and apoMT during zinc metalation. By using a competitive metalation strategy, we have been able to calculate the relative stability constants for each of the seven independent, sequential binding reactions for zinc binding to apoMT. The experimental data indicate that CA out-competes MT only for the three weakest bound zinc atoms—these are the last zinc to bind to the MT. The fractional zinc occupancies in terms of the speciation for each of the 10 species that coexist during the titration were reported and modeled by simulations involving 8 competitive bimolecular reactions. The change in fractional zinc metalation of the apoCA as a function of zinc added to the mixture of apoCA and apoMT was shown to mirror the relative values of the binding affinities for the 7 MT sites. These data provide a detailed and sensitive indication of the buffering role of ZnMT both in providing a zinc sink and in delivering zinc to a zinc-dependent enzyme.

■ ASSOCIATED CONTENT

Supporting Information

Charge state ESI mass spectral data of the competitive zinc titration used to generate the deconvoluted data from Figure 1. Overlaid fits of experimental and modeled data sets of the competitive titration shown in Figures 2 and 3. This material is available free of charge via the Internet at http://pubs.acs.org.

■ AUTHOR INFORMATION

Corresponding Author

*Phone: (519) 661-3821. Fax: (519) 661-3022. E-mail: martin.stillman@uwo.ca.

Funding

We gratefully acknowledge financial support from the National Research Council of Canada through a PGSD award to T.B.J.P. and through Discovery and Research Tools in Instruments Grants to M.J.S.

Notes

The authors declare no competing financial interest.

■ ACKNOWLEDGMENTS

We wish to thank Mr. Doug Hairsine for excellent technical assistance with our mass spectrometers over many years. We wish to acknowledge and thank Dr. Duncan Sutherland for assistance with the simulation calculations and Dr. Michael Tiedemann for helpful discussion.

■ ABBREVIATIONS

ESI-MS, electrospray ionization mass spectrometry; MT, metallothionein; CA, carbonic anhydride; hMT1A, recombinantly prepared human metallothionein 1A; MTF, metal

regulatory transcription factors; SEC, size exclusion chromatography; MWCO, molecular weight cutoff

REFERENCES

(1) Andreini, C., Bertini, I., Cavallaro, G., Holliday, G., and Thornton, J. (2008) Metal ions in biological catalysis: from enzyme databases to general principles. *J. Biol. Inorg. Chem. 13*, 1205−1218.

(2) Andreini, C., Cavallaro, G., Lorenzini, S., and Rosato, A. (2013) MetalPDB: a database of metal sites in biological macromolecular structures. *Nucleic Acids Res. 41*, D312−D319.

(3) Krężel, A., and Maret, W. (2006) Zinc-buffering capacity of a eukaryotic cell at physiological pZn. *J. Biol. Inorg. Chem. 11*, 1049−1062.

(4) Outten, C. E., O'Halloran, and V, T. (2001) Femtomolar Sensitivity of Metalloregulatory Proteins Controlling Zinc Homeostasis. *Science 292*, 2488−2492.

(5) Laity, J. H., and Andrews, G. K. (2007) Understanding the mechanisms of zinc-sensing by metal-response element binding transcription factor-1 (MTF-1). *Arch. Biochem. Biophys. 463*, 201−210.

(6) McMahon, R. J., and Cousins, R. J. (1998) Mammalian Zinc Transporters. *J. Nutr. 128*, 667−670.

(7) Robinson, N., and Pohl, E. (2013) Zinc Sensors in Bacteria, in *Encyclopedia of Metalloproteins* (Kretsinger, R., Uversky, V., and Permyakov, E., Eds.), pp 2499−2506, Springer, New York.

(8) Cousins, R. J., Liuzzi, J. P., and Lichten, L. A. (2006) Mammalian Zinc Transport, Trafficking, and Signals. *J. Biol. Chem. 281*, 24085−24089.

(9) Eide, D. J. (2006) Zinc transporters and the cellular trafficking of zinc. *Biochim. Biophys. Acta, Mol. Cell Res. 1763*, 711−722.

(10) Colvin, R. A., Holmes, W. R., Fontaine, C. P., and Maret, W. (2010) Cytosolic zinc buffering and muffling: their role in intracellular zinc homeostasis. *Metallomics 2*, 306−317.

(11) Tottey, S., Harvie, D. R., and Robinson, N. J. (2005) Understanding How Cells Allocate Metals Using Metal Sensors and Metallochaperones. *Acc. Chem. Res. 38*, 775−783.

(12) Waldron, K. J., Rutherford, J. C., Ford, D., and Robinson, N. J. (2009) Metalloproteins and metal sensing. *Nature 460*, 823−830.

(13) Kulkarni, P. P., She, Y. M., Smith, S. D., Roberts, E. A., and Sarkar, B. (2006) Proteomics of Metal Transport and Metal-Associated Diseases. *Chem.—Eur. J. 12*, 2410−2422.

(14) Nelson, N. (1999) Metal ion transporters and homeostasis. *EMBO J. 18*, 4361−4371.

(15) Taylor, K. M., Vichova, P., Jordan, N., Hiscox, S., Hendley, R., and Nicholson, R. I. (2008) ZIP7-Mediated Intracellular Zinc Transport Contributes to Aberrant Growth Factor Signaling in Antihormone-Resistant Breast Cancer Cells. *Endocrinology 149*, 4912−4920.

(16) Fukada, T., Yamasaki, S., Nishida, K., Murakami, M., and Hirano, T. (2011) Zinc homeostasis and signaling in health and diseases. *J. Biol. Inorg. Chem. 16*, 1123−1134.

(17) Yamasaki, S., Sakata-Sogawa, K., Hasegawa, A., Suzuki, T., Kabu, K., Sato, E., Kurosaki, T., Yamashita, S., Tokunaga, M., and Nishida, K. (2007) Zinc is a novel intracellular second messenger. *J. Cell Biol. 177*, 637−645.

(18) Kang, Y. J. (2006) Metallothionein Redox Cycle and Function. *Exp. Biol. Med. 231*, 1459−1467.

(19) Maret, W., and Vallee, B. L. (1998) Thiolate ligands in metallothionein confer redox activity on zinc clusters. *Proc. Natl. Acad. Sci. U. S. A. 95*, 3478−3482.

(20) Thirumoorthy, N., Shyam Sunder, A., Manisenthil Kumar, K., Senthil Kumar, M., Ganesh, G., and Chatterjee, M. (2011) A review of metallothionein isoforms and their role in pathophysiology. *World J. Surg. Oncol. 9*, 54.

(21) Robbins, A., McRee, D., Williamson, M., Collett, S., Xuong, N., Furey, W., Wang, B., and Stout, C. (1991) Refined crystal structure of Cd, Zn metallothionein at 2.0 Å resolution. *J. Mol. Biol. 221*, 1269−1293.

(22) Coyle, P., Philcox, J., Carey, L., and Rofe, A. (2002) Metallothionein: the multipurpose protein. *Cell. Mol. Life Sc. CMLS 59*, 627−647.

(23) Meloni, G., Sonois, V., Delaine, T., Guilloreau, L., Gillet, A., Teissié, J., Faller, P., and Vašák, M. (2008) Metal swap between Zn7-metallothionein-3 and amyloid-β−Cu protects against amyloid-β toxicity. *Nat. Chem. Biol. 4*, 366−372.

(24) Petering, D. H., Zhu, J., Krezoski, S., Meeusen, J., Kiekenbush, C., Krull, S., Specher, T., and Dughish, M. (2006) Apo-Metallothionein Emerging as a Major Player in the Cellular Activities of Metallothionein. *Exp. Biol. Med. 231*, 1528−1534.

(25) Zalewska, M., Trefon, J., and Milnerowicz, H. (2014) The role of metallothionein interactions with other proteins. *Proteomics 14*, 1343−1356.

(26) Mason, A. Z., Moeller, R., Thrippleton, K. A., and Lloyd, D. (2007) Use of stable isotopically enriched proteins and directly coupled high-performance liquid chromatography inductively coupled plasma mass spectrometry for quantitatively monitoring the transfer of metals between proteins. *Anal. Biochem. 369*, 87−104.

(27) Zaia, J., Fabris, D., Wei, D., Karpel, R. L., and Fenselau, C. (1998) Monitoring metal ion flux in reactions of metallothionein and drug-modified metallothionein by electrospray mass spectrometry. *Protein Sci. 7*, 2398−2404.

(28) Jacob, C., Maret, W., and Vallee, B. L. (1998) Control of zinc transfer between thionein, metallothionein, and zinc proteins. *Proc. Natl. Acad. Sci. U. S. A. 95*, 3489−3494.

(29) Jiang, L.-J., Maret, W., and Vallee, B. L. (1998) The glutathione redox couple modulates zinc transfer from metallothionein to zinc-depleted sorbitol dehydrogenase. *Proc. Natl. Acad. Sci. U. S. A. 95*, 3483−3488.

(30) Feng, W., Cai, J., Pierce, W. M., Franklin, R. B., Maret, W., Benz, F. W., and Kang, Y. J. (2005) Metallothionein transfers zinc to mitochondrial aconitase through a direct interaction in mouse hearts. *Biochem. Biophys. Res. Commun. 332*, 853−858.

(31) Leszczyszyn, O. I., and Blindauer, C. A. (2010) Zinc transfer from the embryo-specific metallothionein EC from wheat: a case study. *Phys. Chem. Chem. Phys. 12*, 13408−13418.

(32) Li, T.-Y., Kraker, A. J., Shaw, C. F., and Petering, D. H. (1980) Ligand substitution reactions of metallothioneins with EDTA and apocarbonic anhydrase. *Proc. Natl. Acad. Sci. U. S. A. 77*, 6334−6338.

(33) Udom, A. O., and Brady, F. O. (1980) Reactivation *in vitro* of zinc-requiring apo-enzymes by rat liver zinc-thionein. *Biochem. J. 187*, 329−335.

(34) Lindskog, S., and Malmström, B. G. (1962) Metal Binding and Catalytic Activity in Bovine Carbonic Anhydrase. *J. Biol. Chem. 237*, 1129−1137.

(35) Kiefer, L. L., Krebs, J. F., Paterno, S. A., and Fierke, C. A. (1993) Engineering a cysteine ligand into the zinc binding site of human carbonic anhydrase II. *Biochemistry 32*, 9896−9900.

(36) Palmiter, R. D., and Findley, S. D. (1995) Cloning and functional characterization of a mammalian zinc transporter that confers resistance to zinc. *EMBO J. 14*, 639.

(37) Wommer, S., Rival, S., Heinz, U., Galleni, M., Frère, J.-M., Franceschini, N., Amicosante, G., Rasmussen, B., Bauer, R., and Adolph, H.-W. (2002) Substrate-activated zinc binding of metallo-β-lactamases: Physiological importance of the mononuclear enzymes. *J. Biol. Chem. 277*, 24142−24147.

(38) Antala, S., and Dempski, R. E. (2012) The Human ZIP4 Transporter Has Two Distinct Binding Affinities and Mediates Transport of Multiple Transition Metals. *Biochemistry 51*, 963−973.

(39) Sharif, R., Thomas, P., Zalewski, P., and Fenech, M. (2012) Zinc deficiency or excess within the physiological range increases genome instability and cytotoxicity, respectively, in human oral keratinocyte cells. *Genes Nutr. 7*, 139−154.

(40) Krężel, A., and Maret, W. (2007) Dual Nanomolar and Picomolar Zn(II) Binding Properties of Metallothionein. *J. Am. Chem. Soc. 129*, 10911−10921.

(41) Namdarghanbari, M. A., Meeusen, J., Bachowski, G., Giebel, N., Johnson, J., and Petering, D. H. (2010) Reaction of the zinc sensor

FluoZin-3 with Zn_7-metallothionein: Inquiry into the existence of a proposed weak binding site. *J. Inorg. Biochem. 104*, 224−231.
(42) Ejnik, J., Muñoz, A., Gan, T., Shaw Iii, C. F., and Petering, D. (1999) Interprotein metal ion exchange between cadmium-carbonic anhydrase and apo-or zinc-metallothionein. *J. Biol. Inorg. Chem. 4*, 784−790.
(43) Petering, D. H., Zhu, J., Krezoski, S., Meeusen, J., Kiekenbush, C., Krull, S., Specher, T., and Dughish, M. (2006) Apo-Metallothionein Emerging as a Major Player in the Cellular Activities of Metallothionein. *Exp. Biol. Med. 231*, 1528−1534.
(44) Summers, K. L., Sutherland, D. E. K., and Stillman, M. J. (2013) Single-Domain Metallothioneins: Evidence of the Onset of Clustered Metal Binding Domains in Zn-rhMT 1a. *Biochemistry 52*, 2461−2471.
(45) Sutherland, D. E. K., Summers, K. L., and Stillman, M. J. (2012) Noncooperative Metalation of Metallothionein 1a and Its Isolated Domains with Zinc. *Biochemistry 51*, 6690−6700.
(46) Sutherland, D. E., and Stillman, M. J. (2014) Challenging conventional wisdom: single domain metallothioneins. *Metallomics 6*, 702.
(47) Avvaru, B. S., Busby, S. A., Chalmers, M. J., Griffin, P. R., Venkatakrishnan, B., Agbandje-McKenna, M., Silverman, D. N., and McKenna, R. (2009) Apo-human carbonic anhydrase II revisited: implications of the loss of a metal in protein structure, stability, and solvent network. *Biochemistry 48*, 7365−7372.
(48) Chan, J., Huang, Z., Watt, I., Kille, P., and Stillman, M. (2008) Metallobiological Necklaces: Mass Spectrometric and Molecular Modeling Study of Metallation in Concatenated Domains of Metallothionein. *Chem.—Eur. J. 14*, 7579−7593.
(49) Hunt, J. B., Rhee, M.-J., and Storm, C. B. (1977) A rapid and convenient preparation of apocarbonic anhydrase. *Anal. Biochem. 79*, 614−617.
(50) Krężel, A., and Maret, W. (2008) Thionein/metallothionein control Zn(II) availability and the activity of enzymes. *J. Biol. Inorg. Chem. 13*, 401−409.
(51) Heinz, U., Kiefer, M., Tholey, A., and Adolph, H.-W. (2005) On the competition for available zinc. *J. Biol. Chem. 280*, 3197−3207.
(52) Ngu, T. T., Easton, A., and Stillman, M. J. (2008) Kinetic Analysis of Arsenic−Metalation of Human Metallothionein: Significance of the Two-Domain Structure. *J. Am. Chem. Soc. 130*, 17016−17028.
(53) Irvine, G. W., and Stillman, M. J. (2013) Topographical analysis of As-induced folding of α-MT1a. *Biochem. Biophys. Res. Commun. 441*, 208−213.
(54) Hong, S.-H., and Maret, W. (2003) A fluorescence resonance energy transfer sensor for the β-domain of metallothionein. *Proc. Natl. Acad. Sci. U. S. A. 100*, 2255−2260.
(55) Irvine, G. W., Summers, K. L., and Stillman, M. J. (2013) Cysteine accessibility during As3+ metalation of the α- and β-domains of recombinant human MT1a. *Biochem. Biophys. Res. Commun. 433*, 477−483.
(56) Palmiter, R. D., Cole, T. B., and Findley, S. D. (1996) ZnT-2, a mammalian protein that confers resistance to zinc by facilitating vesicular sequestration. *EMBO J. 15*, 1784.
(57) Rink, L., and Haase, H. (2007) Zinc homeostasis and immunity. *Trends Immunol. 28*, 1−4.